23rd International Conference
ENGINEERING MECHANICS 2017
Svratka, Czech Republic, 15 – 18 May 2017

THE DYNAMICS OF THE GUIDE ARRANGEMENT BEING AN ELEMENT OF THE LAUNCHER INSTALLED ON A COMBAT VEHICLE

Z. Dziopa*, M. Nyckowski**

Abstract: *The guide arrangement is an element of the self-propelled anti-aircraft missile set. The disturbance which is transferred onto the assembly is generated during the motion of the short-range target homing missiles along the guide. The aim of the paper is to discuss how the input generated within the assembly affects the motion of the guide arrangement.*

Keywords: Guides arrangement, Launcher, Operator, Combat vehicle, Missile, Dynamics.

1. Introduction

The key role in the functioning of the self-propelled anti-aircraft missile set belongs to the arrangement of guides, Fig. 1. Before and at the initial stage of the launching the missile contacts the guide via two directing rings. The missiles moves along the guide simultaneously revolving around the longitudinal axis. At this stage the missile has two points of contact with the launcher guide. These points are represented by two supports. The placement of the directing rings on the missile body determine the location of the supports. The structure of the arrangement results from the accepted assumption and determines missile mobility. The two-point support is binding until the instant the first directing ring of the missile abandons the guide. From that moment the kinematic pair: guide-missile, previously a set with a two-degree freedom, becomes a set with a three-degree freedom of movement. The structure of the arrangement changes as the missile moves along the guide. The support is reduced to one point. In the general case the support leads to the lack of co-linearity of the points located on the longitudinal axis of the missile compared to the points located on the longitudinal axis of the guide. This particular property is characteristic of the arrangement: guide-missile with a three-degree freedom. The fact that the longitudinal axis of the missile and the longitudinal axis of the guide do not overlap all the time is typical of the structure.

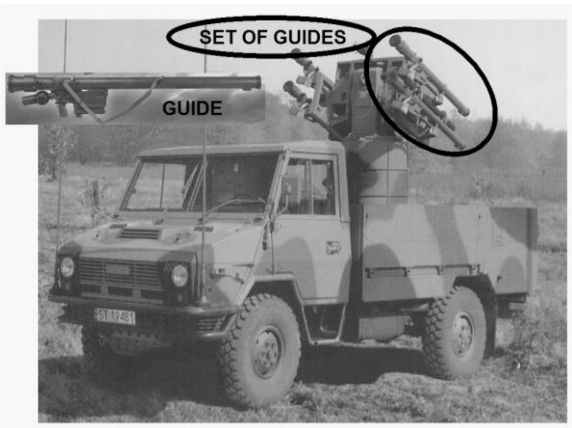

Fig. 1: Self-propelled anti-aircraft missile set.

* Prof. Zbigniew Dziopa, PhD. Eng.: Faculty of Mechatronics and Mechanical Engineering, Kielce University of Technology, al. 1000-lecia P.P. 7; 25-314, Kielce; PL, zdziopa@tu.kielce.pl

** Research Assistant Maciej Nyckowski, MSc. Eng.: Institute of Aviation, al. Krakowska 110/114, 02-256 Warsaw; PL, nyckowski@gmail.com

The guide arrangement consists of two guides located one under the other and links the platform and the missile. It is necessary for the guide arrangement, with maximum efficiency, to insulate the missile against undesirable platform vibrations and disturbance generated by launching missiles as well as providing conditions for proper localization of the target by missiles (Dziopa, 2015).

2. Physical model

The model of the self-propelled anti-aircraft missile assembly consists of five elements (Dziopa, et al 2015). These elements are: a combat vehicle, an operator seated in the chair, a launcher and two missiles and a target. The launcher, which consists of a platform and a set of guides, is installed on the vehicle, Fig. 2.

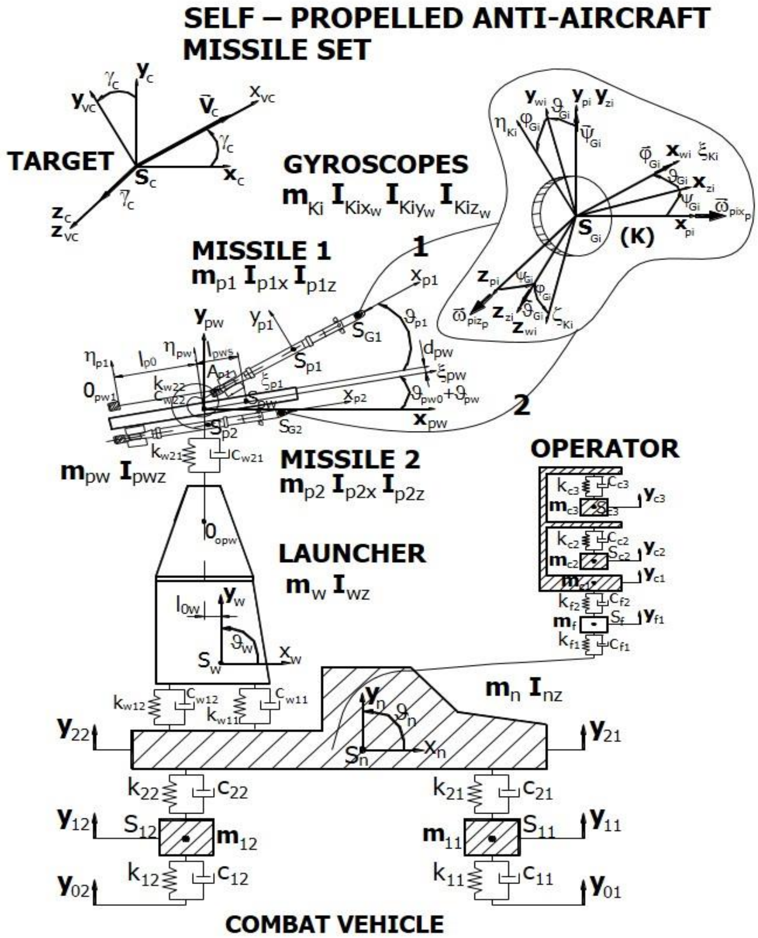

Fig. 2: Physical model of the self-propelled anti-aircraft missile set.

The launcher does not change its configuration after the guide arrangement has been set into the position of intercepting the target (Dziopa, 2013). At this instant the guide arrangement is turned towards the platform in accordance with the elevator angle: ϑ_{pw0}. The ϑ_{pw0} angle is the initial angle of inclination of the set of guides. The guide arrangement is a perfectly rigid body with mass: m_{pw} and the moment of inertia: I_{pwz} (Chatys, 2013). The object is placed on the platform with the use of two passive elastic-damping elements with linear parameters k_{w21} and c_{w21} respectively and k_{w22} and c_{w22}. Two independent generalized coordinates were used to determine the position of the guide arrangement at any moment:

- y_{pw} - vertical relocation of the rotation centre 0_{opw} of the guide arrangement,
- ϑ_{pw} - angle of rotation of the guide arrangement around the $0_{opw} z_{pw}$ axis.

3. Mathematical model

The studied arrangement is described by differential equations with ordinary derivatives represented by twenty-four independent generalized coordinates (Baranowski et al., 2016). On account of the limited number of pages and a lengthy notation of the equations, only the dependences describing the guide arrangement motion will be presented.

The equations representing the motion of the guide arrangement:

$$\begin{aligned}&\left(m_{pw}+m_{p1}+m_{p2}\right)\ddot{y}_{pw}+[m_{pw}l_{03}+m_{p1}\left(l_{15}-l_{06}-l_{14}+l_{11}\right)+\\&+m_{p2}\left(l_{25}+l_{06}+l_{24}+l_{21}\right)]\ddot{\vartheta}_{pw}+m_{p1}\left(l_{11}-l_{14}\right)\ddot{\vartheta}_{p1}+m_{p2}\left(l_{21}-l_{24}\right)\ddot{\vartheta}_{p2}+\\&+m_{p1}l_{02}\ddot{\xi}_{p1}+m_{p2}l_{02}\ddot{\xi}_{p2}+[m_{pw}l_{04}+m_{p1}\left(l_{16}+l_{05}+l_{13}+l_{12}\right)+\\&+m_{p2}\left(l_{26}-l_{05}-l_{23}+l_{22}\right)]\dot{\vartheta}_{pw}^{2}-m_{p1}\left(l_{12}+l_{13}\right)\dot{\vartheta}_{p1}^{2}-m_{p2}\left(l_{22}-l_{23}\right)\dot{\vartheta}_{p2}^{2}+\\&-2m_{p1}\left(l_{13}+l_{12}\right)\dot{\vartheta}_{pw}\dot{\vartheta}_{p1}+2m_{p2}\left(l_{23}-l_{22}\right)\dot{\vartheta}_{pw}\dot{\vartheta}_{p2}+2m_{p1}l_{01}\dot{\vartheta}_{pw}\dot{\xi}_{p1}+\\&+2m_{p2}l_{01}\dot{\vartheta}_{pw}\dot{\xi}_{p2}+k_{w21}\lambda_{w21}=\left(P_{ss1}\sin\vartheta_{p1}+P_{ss2}\sin\vartheta_{p2}\right)\cos\left(\vartheta_{pw0}+\vartheta_{pw}\right)+\\&-\left(m_{pw}+m_{p1}+m_{p2}\right)g\end{aligned} \tag{1}$$

$$\begin{aligned}&\left(m_{pw}l_{pws}^{2}+I_{pw}+m_{p1}a_{11}+I_{p1}+m_{p2}a_{21}+I_{p2}\right)\ddot{\vartheta}_{pw}+[m_{pw}l_{03}+\\&+m_{p1}\left(l_{15}-l_{06}-l_{14}+l_{11}\right)+m_{p2}\left(l_{25}-l_{06}-l_{24}+l_{21}\right)]\ddot{y}_{pw}+\left(m_{p1}a_{13}+I_{p1}\right)\ddot{\vartheta}_{p1}+\\&+\left(m_{p2}a_{23}+I_{p2}\right)\ddot{\vartheta}_{p2}-m_{p1}a_{12}\ddot{\xi}_{p1}+m_{p2}a_{22}\ddot{\xi}_{p2}-m_{p1}a_{14}\dot{\vartheta}_{p1}^{2}-m_{p2}a_{24}\dot{\vartheta}_{p2}^{2}+\\&-2m_{p1}a_{14}\dot{\vartheta}_{pw}\dot{\vartheta}_{p1}-2m_{p2}a_{24}\dot{\vartheta}_{pw}\dot{\vartheta}_{p2}+2m_{p1}a_{15}\dot{\vartheta}_{pw}\dot{\xi}_{p1}+2m_{p2}a_{25}\dot{\vartheta}_{pw}\dot{\xi}_{p2}+\\&+k_{w22}\lambda_{w22}=P_{ss1}\left(\xi_{p1}-l_{p0}\right)\sin\vartheta_{p1}+P_{ss2}\left(\xi_{p2}-l_{p0}\right)\sin\vartheta_{p2}+\\&+m_{p1}g\left(l_{06}-l_{15}+l_{14}-l_{11}\right)-m_{p2}g\left(l_{06}+l_{25}+l_{24}-l_{21}\right)-m_{pw}gl_{03}\end{aligned} \tag{2}$$

where:

$$\lambda_{w21}=y_{pw}+y_{pwst}+l_{0w}\left(\vartheta_{w}+\vartheta_{wst}\right)-\left(y_{w}+y_{wst}\right),\qquad \lambda_{w22}=\vartheta_{pw}+\vartheta_{pwst}-\left(\vartheta_{w}+\vartheta_{wst}\right)$$

$$l_{01}=\cos\left(\vartheta_{pw0}+\vartheta_{pw}\right),\ l_{02}=\sin\left(\vartheta_{pw0}+\vartheta_{pw}\right),\ l_{03}=l_{pws}\cos\left(\vartheta_{pw0}+\vartheta_{pw}\right),\ l_{04}=l_{pws}\sin\left(\vartheta_{pw0}+\vartheta_{pw}\right)$$

$$l_{05}=d_{pw}\cos\left(\vartheta_{pw0}+\vartheta_{pw}\right),\ l_{06}=d_{pw}\sin\left(\vartheta_{pw0}+\vartheta_{pw}\right),\quad l_{11}=l_{ps1}\cos\left(\vartheta_{pw0}+\vartheta_{pw}+\vartheta_{p1}\right)$$

$$l_{12}=l_{ps1}\sin\left(\vartheta_{pw0}+\vartheta_{pw}+\vartheta_{p1}\right),\ l_{13}=d_{p}\cos\left(\vartheta_{pw0}+\vartheta_{pw}+\vartheta_{p1}\right),\ l_{14}=d_{p}\sin\left(\vartheta_{pw0}+\vartheta_{pw}+\vartheta_{p1}\right)$$

$$l_{15}=\left(\xi_{p1}-l_{p0}\right)\cos\left(\vartheta_{pw0}+\vartheta_{pw}\right),\ l_{16}=\left(\xi_{p1}-l_{p0}\right)\sin\left(\vartheta_{pw0}+\vartheta_{pw}\right),\ l_{21}=l_{ps2}\cos\left(\vartheta_{pw0}+\vartheta_{pw}+\vartheta_{p2}\right),$$

$$l_{22}=l_{ps2}\sin\left(\vartheta_{pw0}+\vartheta_{pw}+\vartheta_{p2}\right),\ l_{23}=d_{p}\cos\left(\vartheta_{pw0}+\vartheta_{pw}+\vartheta_{p2}\right),\ l_{24}=d_{p}\sin\left(\vartheta_{pw0}+\vartheta_{pw}+\vartheta_{p2}\right)$$

$$l_{25}=\left(\xi_{p2}-l_{p0}\right)\cos\left(\vartheta_{pw0}+\vartheta_{pw}\right),\ l_{26}=\left(\xi_{p2}-l_{p0}\right)\sin\left(\vartheta_{pw0}+\vartheta_{pw}\right)$$

$$\begin{aligned}a_{11}=&\,d_{pw}^{2}+d_{p}^{2}+l_{ps1}^{2}+\left(\xi_{p1}-l_{p0}\right)^{2}+2d_{w}d_{p}\cos\vartheta_{p1}-2d_{p}\left(\xi_{p1}-l_{p0}\right)\sin\vartheta_{p1}+2d_{pw}l_{ps1}\sin\vartheta_{p1}+\\&+2l_{ps1}\left(\xi_{p1}-l_{p0}\right)\cos\vartheta_{p1}\end{aligned}$$

$$a_{12}=d_{pw}+d_{p}\cos\vartheta_{p1}+l_{ps1}\sin\vartheta_{p1},\ a_{22}=d_{pw}+d_{p}\cos\vartheta_{p2}+l_{ps2}\sin\vartheta_{p2}$$

$$a_{13}=d_{p}^{2}+l_{ps1}^{2}+d_{pw}d_{p}\cos\vartheta_{p1}-d_{p}\left(\xi_{p1}-l_{p0}\right)\sin\vartheta_{p1}+d_{pw}l_{ps1}\sin\vartheta_{p1}+l_{ps1}\left(\xi_{p1}-l_{p0}\right)\cos\vartheta_{p1}$$

$$a_{14}=d_{pw}d_{p}\sin\vartheta_{p1}+d_{p}(\xi_{p1}-l_{p0})\cos\vartheta_{p1}-d_{pw}l_{ps1}\cos\vartheta_{p1}+l_{ps1}(\xi_{p1}-l_{p0})\sin\vartheta_{p1}$$

$$a_{15}=\xi_{p1}-l_{p0}-d_{p}\sin\vartheta_{p1}+l_{ps1}\cos\vartheta_{p1}$$

$$\begin{aligned}a_{21}=&\,d_{pw}^{2}+d_{p}^{2}+l_{ps2}^{2}+\left(\xi_{p2}-l_{p0}\right)^{2}+2d_{pw}d_{p}\cos\vartheta_{p2}-2d_{p}\left(\xi_{p2}-l_{p0}\right)\sin\vartheta_{p2}+2d_{pw}l_{ps2}\sin\vartheta_{p2}+\\&+2l_{ps2}\left(\xi_{p2}-l_{p0}\right)\cos\vartheta_{p2}\end{aligned}$$

$$a_{22}=d_{pw}+d_{p}\cos\vartheta_{p2}+l_{ps2}\sin\vartheta_{p2},\ a_{25}=\xi_{p2}-l_{p0}-d_{p}\sin\vartheta_{p2}+l_{ps2}\cos\vartheta_{p2}$$

$$a_{23}=d_{p}^{2}+l_{ps2}^{2}+d_{pw}d_{p}\cos\vartheta_{p2}-d_{p}\left(\xi_{p2}-l_{p0}\right)\sin\vartheta_{p2}+d_{pw}l_{ps2}\sin\vartheta_{p2}+l_{ps2}\left(\xi_{p2}-l_{p0}\right)\cos\vartheta_{p2}$$

$$a_{24}=d_{pw}d_{p}\sin\vartheta_{p2}+d_{p}(\xi_{p2}-l_{p0})\cos\vartheta_{p2}-d_{pw}l_{ps2}\cos\vartheta_{p2}+l_{ps2}(\xi_{p2}-l_{p0})\sin\vartheta_{p2}$$

4. Numerical simulation

The exemplary courses of linear acceleration variation of the guide arrangement are presented in Figs. 3, 4 (two-degree freedom) and 5, 6 (three-degree freedom). The generated disturbance results from the drive of the assembly along a rough road at the speed of $30[\mathrm{km/h}]$ and launching two missiles (Gapiński, 2014). The characteristics for three cases of inclination of the guide arrangement are compared. It is possible to determine such instants of time which represent physical phenomena of mechanical reaction nature in the course of three seconds of the assembly operation (Koruba, 2013 and Stefański, 2012).

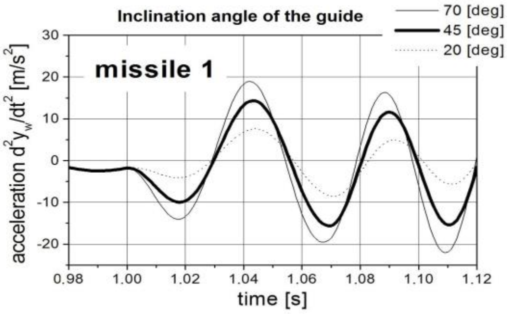

Fig. 3: Take-off missile 1.

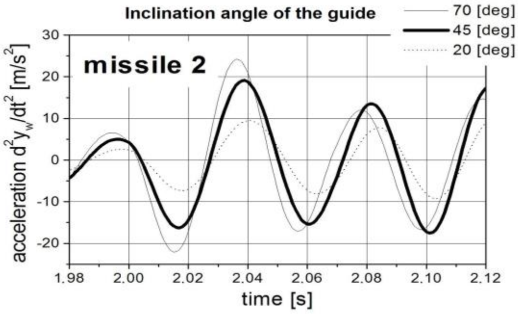

Fig. 4: Take-off missile 2.

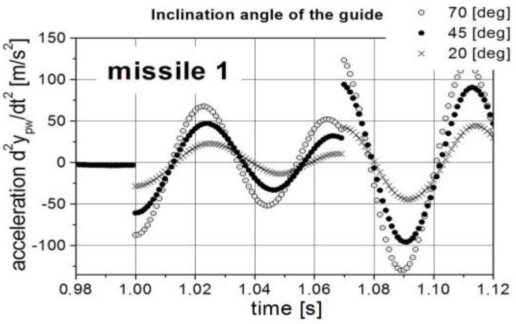

Fig. 5: Take-off missile 1.

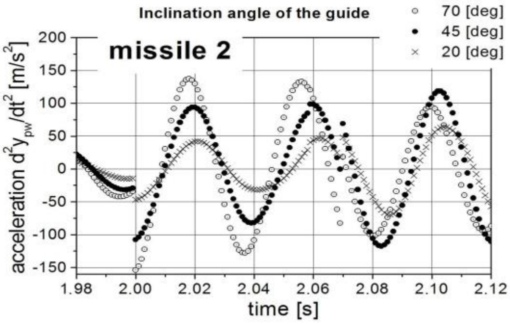

Fig. 6: Take-off missile 2.

5. Conclusions

The guide arrangement suffers from a distinct induction during the movement of the assembly along an uneven road and launching both missiles. The dynamic characteristic of the guide arrangement and their inclination angle determine the level of disturbance which affects the launching missile. A distinct change in the course of alteration of physical quantities describing the motion of the guide arrangement, e.g. the abrupt change of linear acceleration, occurs when the structure of the assembly or its mass is changed.

References

Baranowski, L., Gadomski, B., Majewski, P. and Szymonik, J. (2016) Explicit "ballistic M-model": a refinement of the implicit "modified point mass trajectory model". Bulletin of the Polish Academy of Sciences - Technical Sciences, 64, 1, pp. 81-89, DOI: 10.1515/bpasts-2016-0010.

Chatys, R. (2013) Investigation of the Effect of Distribution of the Static Strength on the Fatigue Failure of a Layered Composite by Using the Markov Chains Theory. Mechanics of Composite Materials, Vol. 48, No. 6, pp. 629-638, (DOI: 10.1007/s11029-013-9307-9, Springer, ISSN 0191-5665).

Dziopa, Z., (2013) Elements of Dynamics Analysis of the Warship Launcher of Anti-Aircraft Short Range Homing Missiles. Solid State Phenomena, vol.196, Mechatronics System, Mechanics and Materials, Trans Tech Publications Ltd, Switzerland, ISBN-13: 978-3-03785-274-3, pp. 28-42.

Dziopa, Z., Buda, P., Nyckowski, M. and Pawlikowski, R. (2015) Dynamics of an unguided missiles launcher. Journal of Theoretical and Applied Mechanics. No. 1, Vol. 53, ISSN 1429-2955, pp. 69-80.

Dziopa, Z. and Koruba, Z. (2015) The impact of launcher turret vibrations control on the rocket launch. Bulletin of the Polish Academy of Sciences – Technical Sciences, Vol. 63, No. 3, pp. 717-728.

Gapinski, D. and Krzysztofik, I. (2014) The process of tracking an air target by the designed scanning and tracking seeker.15th International Carpathian Control Conference (ICCC), Velke Karlovice, Czech Republic, pp. 129-134, IEEE Catalog Number: CFP1442L-CDR, ISBN 978-1-4799-3528-4.

Koruba, Z. and Krzysztofik, I. (2013) An algorithm for selecting optimal controls to determine the estimators of the coefficients of a mathematical model for the dynamics of a self-propelled anti-aircraft missile system. Proceedings of the Institution of Mechanical Engineers, Journal of Multi-Body Dynamics, 227, 1, pp. 12-16.

Stefański, K. and Koruba, Z. (2012) Analysis of the Guiding of Bombs On Ground Targets Using a Gyroscope System. Journal of Theoretical And Applied Mechanics, Vol. 50, Iss. 4, pp. 967-973.